CHIN. PHYS. LETT. Vol. 35, No. 3 (2018) 037501

The Mixed Spin-1/2 and Spin-1 Ising–Heisenberg Model in the Mean-Field Approximation: a New Approach

Erhan Albayrak**

Erciyes University, Department of Physics, Kayseri 38039, Turkey

(Received 28 August 2017)

Thermodynamic properties of the mixed spin-1 and spin-1/2 Ising–Heisenberg model are studied on a honeycomb lattice using a new approach in the mean-field approximation to analyze the effects of longitudinal D_z and transverse D_x crystal fields. The phase diagrams are calculated in detail by studying the thermal variations of the order parameters, i.e., magnetizations and quadrupole moments, and compared with the literature to assess the reliability of the new approach. It is found that the model yields both second- and first-order phase transitions, and tricritical points. The compensation behavior of the model is also investigated for the sublattice magnetizations, and longitudinal and transverse quadrupolar moments. The latter type of compensation is observed in the literature but its possible importance is overlooked.

PACS: 75.10.Jm, 75.30.Kz, 05.50.+q DOI: 10.1088/0256-307X/35/3/037501

Research of the mixed spin-1/2 and spin-1 Ising model is generally considered as the first step into the analysis of mixed-spin systems, since it involves the possible lowest spin values with fewer states. Therefore, it has attracted a great deal of attention. It has been examined with different spin configurations to study its physical properties using numerous techniques.

In most of these works, the Hamiltonian contains only a longitudinal crystal field (LCF) which is usually taken along the z-axis. It is well-known that as D_z becomes more negative, the system is driven to its lowest spin values because of its competition with the bilinear exchange interaction parameter. Lately, the effects of the transverse crystal field (TCF) (D_x), i.e., along the x-axis, have also been receiving attention. It is found that the existence of D_x also does affect the critical behavior of the system. Most of these works use different forms of effective field theory (EFT), such as the critical behaviors of a mixed spin-1/2 and spin-$s_{\rm B}$ Ising system with TCF D_x,[1] the bond-diluted mixed spin-1/2 and spin-1 Ising model with uniaxial and biaxial single-ion anisotropy on a simple cubic structure,[2] the ferrimagnetic multilayer system consisting of L layers of spin-1/2 atoms, L layers of spin-1 atoms and a disordered interface between them,[3] the critical temperature and the layer longitudinal magnetizations of a ferromagnetic (FM) or ferrimagnetic mixed Ising bilayer system with both spin-1/2 and spin-1 (or spin-32) in a TCF,[4] the FM or ferrimagnetic bilayer system consisting of two magnetic monolayers with different spins ($S_{\rm A} = 1/2$ and $S_{\rm B} = 1, 3/2$) and different interaction constants coupled together in a TCF,[5] the critical behaviors of the TCF and bimodal magnetic field mixed spin-1/2 and spin-1 Ising model with bond dilution or percolation threshold on a simple cubic lattice,[6] and the compensation behaviors of mixed spin-1/2 and spin-1 Ising model with a TCF in an external magnetic field on a simple cubic lattice.[7] In addition, the mixed spin-1/2 and spin-1 Ising chain with both LCF and TCF was solved exactly by means of a mapping to the spin-1/2 Ising chains with alternating transverse fields and the Jordan–Wigner transformation,[8] and the FM spin-1 Ising model with a TCF term was investigated by means of a mapping to the usual spin-1/2 transverse Ising model.[9]

The addition of transverse spin components to the longitudinal ones leads to a quantum mechanical system since the components of spin operators do not commute with each other. Thus the spin systems are intrinsically quantum mechanical and are usually studied in the Heisenberg models. The case with mixed spin-1 and spin-1/2 was examined in some works. For example, the effects of both an exchange and a single-ion anisotropy were investigated, using the Oguchi approximation to study its phase diagrams[10] and compensation temperatures.[11] The ground-state and finite-temperature behavior[12] and phase transitions[13] on decorated planar lattices consisting of interconnected diamonds were investigated within the framework of generalized decoration-iteration transformation, the magnetic properties on a two-dimensional square lattice were investigated by means of the double-time Green's function technique within the random phase decoupling approximation,[14] and the geometric frustration in the mixed spin-1/2 and spin-S Ising–Heisenberg diamond chains was investigated by combining the Kambe projection method, decoration-iteration transformation and the transfer-matrix method.[15] In addition to these works, we can also mention a few others,

**Corresponding author. Email: albayrak@erciyes.edu.tr

© 2018 Chinese Physical Society and IOP Publishing Ltd

e.g., the compensation point of the ferrimagnetic systems described by the Heisenberg Hamiltonian with exchange anisotropy instead of single-ion anisotropy was analyzed,[16] and the exchange anisotropy and crystal field effects for the mixed spin-2 and spin-1/2 were studied on square and simple cubic lattices using the Oguchi approximation.[17]

It should be mentioned that one needs to make assumptions or approximations to obtain some reliable solutions in both the Ising and the Heisenberg models. For example, the Oguchi approximation is not useful at low temperatures[17,18] and its results are only valid for the spins on a simple cubic lattice because of the Mermin–Wagner theorem.[19] In this work, the mixed spin-1/2 and spin-1 Ising–Heisenberg model under the influence of LCF, TCF, bilinear exchange interaction and longitudinal external magnetic field is studied on a honeycomb lattice with a new assumption, which is valid for the mixed-spin systems in the MF. This new approach is introduced to obtain better results using simple calculations in agreement with the literature.

The usual Hamiltonian including the TCF effects for the mixed spin-1/2 and spin-1 system may be given as

$$\begin{aligned}\hat{\mathcal{H}} = & -J\sum_{\langle ij\rangle}\hat{S}^z_{i\mathrm{A}}\hat{S}^z_{j\mathrm{B}} - D_z\sum_{j\in\mathrm{B}}(\hat{S}^z_{j\mathrm{B}})^2 \\ & - D_x\sum_{j\in\mathrm{B}}(\hat{S}^x_{j\mathrm{B}})^2 - h_{\mathrm{A}}\sum_{i\in\mathrm{A}}\hat{S}^z_{i\mathrm{A}} - h_{\mathrm{B}}\sum_{j\in\mathrm{B}}\hat{S}^z_{j\mathrm{B}}, \quad (1)\end{aligned}$$

where $S^{\delta}_{i\mathrm{A}}$ and $S^{\delta}_{j\mathrm{B}}$ with $(\delta = x, z)$ are the components of spin-1/2 and spin-1 operators for the sublattices A and B, respectively, D_x and D_z are the TCF and LCF parameters acting only to the spin-1 sites, i.e., only on sublattice B, J is the nearest-neighbor (NN) bilinear exchange interaction parameter, h_{A} and h_{B} are the longitudinal external magnetic fields on the sublattices which are set equal to zero eventually to obtain the spontaneous values of order parameters.

The Hamiltonian $\hat{\mathcal{H}}$ in Eq. (1) is written using the mean-field approximation (MFA) as

$$-\beta\hat{\mathcal{H}} = -\beta\sum_{ij}\hat{\mathcal{H}}^{(ij)}_{\mathrm{MFA}}, \quad (2)$$

where the NN pair interactions between the spin components are approximated, and the rest of the interactions are treated exactly. Note that in ordinary MFA, the NN pair interactions between the spin components are treated exactly and the rest of the interactions are replaced with the effective field terms,[10,11,17,18] here we employ an opposite approximation. Thus in this approximation the Hamiltonian is given as

$$\begin{aligned}-\beta\hat{\mathcal{H}}^{(ij)}_{\mathrm{MFA}} = & \beta Jz[M^z_{1/2}\hat{S}^z_{j\mathrm{B}} + M^z_1\hat{S}^z_{i\mathrm{A}}] + \beta D_z(\hat{S}^z_{j\mathrm{B}})^2 \\ & + \beta D_x(\hat{S}^x_{j\mathrm{B}})^2 + \beta h_{\mathrm{A}}\hat{S}^z_{i\mathrm{A}} + \beta h_{\mathrm{B}}\hat{S}^z_{j\mathrm{B}}, \quad (3)\end{aligned}$$

where the first term of Eq. (1) is replaced with the term $z[M^z_{1/2}\hat{S}^z_{j\mathrm{B}} + M^z_1\hat{S}^z_{i\mathrm{A}}]$ for our new approach in the MF case. Note also that in our approach h_{A} and h_{B} were taken as the external magnetic fields in contrary to Refs. [10,11,17,18], where they are taken as the MF terms. Here $M^z_{1/2} = \langle\hat{S}^z_{i\mathrm{A}}\rangle$ and $M^z_1 = \langle\hat{S}^z_{j\mathrm{B}}\rangle$ are the magnetizations of the sublattices, z is the number of NNs, i.e., the coordination number, and $\langle\ldots\rangle$ corresponds to thermal averages. The spin operators are given for the spin-1/2 and spin-1 as

$$\begin{aligned}&\hat{S}^z_{i\mathrm{A}} = \frac{1}{2}\begin{pmatrix}1 & 0\\ 0 & -1\end{pmatrix},\ \hat{S}^z_{j\mathrm{B}} = \begin{pmatrix}1 & 0 & 0\\ 0 & 0 & 0\\ 0 & 0 & -1\end{pmatrix},\\ &\hat{S}^x_{j\mathrm{B}} = \frac{1}{\sqrt{2}}\begin{pmatrix}0 & 1 & 0\\ 1 & 0 & 1\\ 0 & 1 & 0\end{pmatrix},\ (\hat{S}^z_{j\mathrm{B}})^2 = \begin{pmatrix}1 & 0 & 0\\ 0 & 0 & 0\\ 0 & 0 & 1\end{pmatrix},\\ &(\hat{S}^x_{j\mathrm{B}})^2 = \frac{1}{2}\begin{pmatrix}1 & 0 & 1\\ 0 & 2 & 0\\ 1 & 0 & 1\end{pmatrix}. \quad (4)\end{aligned}$$

Since $\hat{S}_{i\mathrm{A}}$ and $\hat{S}_{j\mathrm{B}}$ belong to different spaces with different degrees, they need a special product called the direct product with unitary matrices $\boldsymbol{I}_{2\times2}$ and $\boldsymbol{I}_{3\times3}$, respectively, which are given as

$$\boldsymbol{I}_{2\times2} = \begin{pmatrix}1 & 0\\ 0 & 1\end{pmatrix},\ \boldsymbol{I}_{3\times3} = \begin{pmatrix}1 & 0 & 0\\ 0 & 1 & 0\\ 0 & 0 & 1\end{pmatrix}. \quad (5)$$

Thus Eq. (3) should be written in a new form using the direct products as

$$\begin{aligned}-\beta\hat{\mathcal{H}}^{(ij)}_{\mathrm{MFA}} = & \beta Jz[M^z_{1/2}(\hat{S}^z_{j\mathrm{B}}\otimes\boldsymbol{I}_{2\times2}) \\ & + M^z_1(\boldsymbol{I}_{3\times3}\otimes\hat{S}^z_{i\mathrm{A}})] \\ & + \beta D_z(\hat{S}^z_{j\mathrm{B}})^2\otimes\boldsymbol{I}_{2\times2} \\ & + \beta D_x(\hat{S}^x_{j\mathrm{B}})^2\otimes\boldsymbol{I}_{2\times2} \\ & + \beta h_{\mathrm{A}}\boldsymbol{I}_{3\times3}\otimes\hat{S}^z_{i\mathrm{A}} \\ & + \beta h_{\mathrm{B}}\hat{S}^z_{j\mathrm{B}}\otimes\boldsymbol{I}_{2\times2}. \quad (6)\end{aligned}$$

As a result, one can obtain a symmetric matrix in the form

$$\begin{aligned}&-\beta\hat{\mathcal{H}}^{(ij)}_{\mathrm{MFA}} \\ &= \begin{pmatrix}a_{11} & 0 & 0 & 0 & \beta D_x/2 & 0\\ 0 & a_{22} & 0 & 0 & 0 & \beta D_x/2\\ 1 & 0 & a_{33} & 0 & 0 & 0\\ 1 & 0 & 0 & a_{44} & 0 & 0\\ \beta D_x/2 & 0 & 0 & 0 & a_{55} & 0\\ 0 & \beta D_x/2 & 0 & 0 & 0 & a_{66}\end{pmatrix}, \quad (7)\end{aligned}$$

where

$$\begin{aligned}
a_{11} &= \beta(D_x + 2D_z + 2h_{\rm B} + h_{\rm A} \\
&\quad + 2JzM^z_{1/2} + JzM^z_1)/2, \\
a_{22} &= \beta(D_x + 2D_z + 2h_{\rm B} - h_{\rm A} \\
&\quad + 2JzM^z_{1/2} - JzM^z_1)/2, \\
a_{33} &= \beta(2D_x + h_{\rm A} + JzM^z_1)/2, \\
a_{44} &= \beta(2D_x - h_{\rm A} - JzM^z_1)/2, \\
a_{55} &= \beta(D_x + 2D_z - 2h_{\rm B} + h_{\rm A} \\
&\quad - 2JzM^z_{1/2} + JzM^z_1)/2, \\
a_{66} &= \beta(D_x + 2D_z - 2h_{\rm B} - h_{\rm A} \\
&\quad - 2JzM^z_{1/2} - JzM^z_1)/2. \qquad (8)
\end{aligned}$$

In this form, one can easily obtain the eigenvalues of a 6×6 square matrix as

$$\begin{aligned}
&\lambda_{1,2} = \beta(2D_x \pm h_{\rm A} \pm JzM^z_1)/2, \\
&\lambda_{3,4} = \beta(D_x + 2D_z - h_{\rm A} - JzM^z_1 \\
&\pm \sqrt{D^2_x + 4h^2_{\rm B} + 8h_{\rm B}JzM^z_{1/2} + (2JzM^z_{1/2})^2})/2, \\
&\lambda_{5,6} = \beta(D_x + 2D_z + h_{\rm A} + JzM^z_1 \\
&\pm \sqrt{D^2_x + 4h^2_{\rm B} + 8h_{\rm B}JzM^z_{1/2} + (2JzM^z_{1/2})^2})/2. \qquad (9)
\end{aligned}$$

After having calculated the eigenvalues, the rest of the formulation is a standard one. The partition function may be obtained using the six eigenvalues as

$$Z = \sum_{i=1}^{6} e^{\lambda_i}. \qquad (10)$$

The free energy is given by the definition

$$F = -(1/\beta)\ln Z. \qquad (11)$$

The only order parameter belonging to the sublattice A with spin-1/2 is magnetization which is given by

$$M^z_{1/2} = -\frac{\partial F}{\partial h_{\rm A}} = \frac{1}{\beta}\frac{\partial \ln Z}{\partial h_{\rm A}} = \frac{1}{\beta Z}\frac{\partial Z}{\partial h_{\rm A}}. \qquad (12)$$

The spin-1 sites, i.e., sublattice B, have three order parameters: the magnetization, the transverse quadrupole moment and the longitudinal quadrupole moment, which are

$$M^z_1 = -\frac{\partial F}{\partial h_{\rm B}} = \frac{1}{\beta}\frac{\partial \ln Z}{\partial h_{\rm B}} = \frac{1}{\beta Z}\frac{\partial Z}{\partial h_{\rm B}}, \qquad (13)$$

$$Q^x_1 = -\frac{\partial F}{\partial D_x} = \frac{1}{\beta}\frac{\partial \ln Z}{\partial D_x} = \frac{1}{\beta Z}\frac{\partial Z}{\partial D_x}, \qquad (14)$$

$$Q^z_1 = -\frac{\partial F}{\partial D_z} = \frac{1}{\beta}\frac{\partial \ln Z}{\partial D_z} = \frac{1}{\beta Z}\frac{\partial Z}{\partial D_z}. \qquad (15)$$

The explicit forms of these equations are too long to be given here.

To obtain the phase diagrams of our model, one has to study the thermal variations of order parameters. For this purpose, a few of the sample figures are illustrated, which show the existence of some special critical points of our model when external magnetic fields are set to zero. We have also made the changes as $D_z = D$ and $D_x = \Delta$. Figure 1(a) shows that $M^z_{1/2}$ and M^z_1 go to zero at the same second-order phase transition temperature, $T_{\rm c}$, where the quadrupole moments exhibit slight cusps. In addition, Q_x first increases then decreases with increasing temperature, Q_z always decreases with increasing temperature, and they eventually combine at their common limiting values of 2/3. These kinds of thermal behavior of the order parameters are similar with the figures given in Refs. [20–22]. Figure 1(b) is similar with the previous figure, but now a special temperature $T_{{\rm comp},Q}$ is also indicated. Here Q_x and Q_z compensate for each other at this temperature $T_{{\rm comp},Q} < T_{\rm c}$. As far as we know this behavior was observed in Fig. 2 of Ref. [21] but its possible importance, as in the compensation temperatures of magnetizations, was overlooked, and we believe that it could be as important as the compensation temperatures seen for the sublattice magnetizations. Figure 1(c) shows the thermal variations of the order parameters at the first-order phase transition temperature $T_{\rm t}$. As seen $M^z_{1/2}$ and M^z_1 jump to zero, and Q_x and Q_z jump to some other values at $T_{\rm t}$. Figure 1(d) shows the compensation temperature for the sublattice magnetizations at a special temperature $T_{{\rm comp},M} < T_{\rm c}$, at which $M^z_{1/2} = M^z_1$. Here $T_{{\rm comp},Q}$ and $T_{\rm t}$ are also observed.

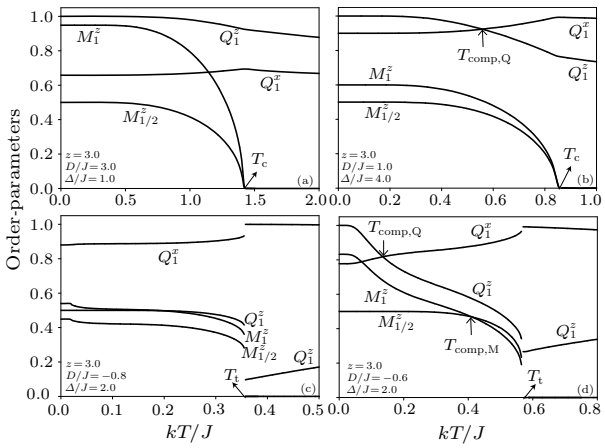

Fig. 1. Thermal variations of order parameters for $z = 3$: (a) obtaining of $T_{\rm c}$ when $D/J = 3.0$ and $\Delta/J = 1.0$, (b) existence of $T_{{\rm comp},Q}$ where Q_x and Q_z curves intersect for $D/J = 1.0$ and $\Delta/J = 4.0$, (c) obtaining of $T_{\rm t}$ when $D/J = -0.8$ and $\Delta/J = 2.0$, and (d) existence of $T_{{\rm comp},M}$ and $T_{{\rm comp},Q}$ for $D/J = -0.6$ and $\Delta/J = 2.0$.

Before illustrating the phase diagrams, we should note that the solid, dashed and dash-dotted lines are used to indicate the second- and first-order phase transition and compensation temperatures, respectively.

In the phase diagrams, we only study $T_{\mathrm{comp},Q}$ since $T_{comp,M}$ has already been studied exhaustively. The filled circles label the tricritical points (TCP) at which the T_{c}- and T_{t} lines meet. It should also be noted that our model must reduce to the well-known mixed-spin Blume–Capel model when $\Delta/J = 0.0$.

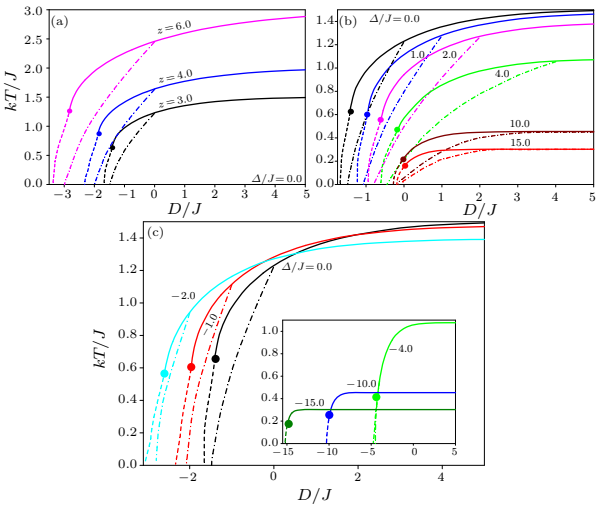

Fig. 2. Phase diagrams on $(D/J, kT/J)$ planes for given Δ/J. The lines always consist of T_{c}- and T_{t} lines combined at TCPs. The $T_{\mathrm{comp},Q}$ lines start from the corresponding T_{c} lines and terminate at $kT/J = 0$. Here (a) $\Delta/J = 0.0$ and $z = 3$, 4 and 6, (b) $\Delta/J = 0.0$, 1.0, 2.0, 4.0, 10.0 and 15.0, and $z = 3$, and (c) $\Delta/J = 0.0$, -1.0, -2.0, -4.0, -10.0 and -15.0, and $z = 3$.

Our first phase diagram, Fig. 2(a), is obtained on the $(D/J, kT/J)$ plane for $\Delta/J = 0.0$ and $z = 3$, 4 and 6 when $h_{\mathrm{A}} = h_{\mathrm{B}} = 0.0$. This will enable us to evaluate the validity of the new approximation used in this work. The phase diagrams exhibit first T_{t} lines at low temperatures and at negative D/J values, then these lines terminate at the TCPs from which the T_{c} lines originate which increase when D/J is increased and become constant at higher D/J at some temperatures for all z values. In addition, the critical lines are seen at higher temperatures for higher z values. These two points are well-known common characteristics of Ising and Heisenberg models. As seen from the figure, the T_{c} lines are at higher temperatures and T_{t} lines extend to higher negative D/J values when compared with the literature. The T_{c} lines become constant for higher positive D/J at $kT/J \cong 1.507$, 2.008 and 3.009 for $z = 3$, 4 and 6, respectively. They are higher, for example, when compared with the results of exact recursion relations on the Bethe lattice,[23] mapping,[24] discrete nonlinear map,[25] numerical matrix study[26] and MF renormalization group[27] and so on. The T_{t} lines of this work terminate at $D/J = -1.6832$, -2.3200 and -3.3760, which are higher than the expected values of -1.5, -2.0 and -3.0 for $z = 3$, 4 and 6, respectively. In addition, the TCPs exist when $z > 4$ in the literature even if there are some controversial results. In this work, we obtain TCPs for all z, which may be caused by overestimating the temperatures of the critical lines. Figure 2(b) is the phase diagram obtained on the $(D/J, kT/J)$ planes for given values of Δ/J with $z = 3$ and $h_{\mathrm{A}} = h_{\mathrm{B}} = 0.0$. As seen from the figure with $\Delta/J = 0.0$, the T_{c} line combines with the T_{t} line at the TCP. The $T_{\mathrm{comp},Q}$ line starts from the T_{c} line and decreases in temperature as Δ/J becomes more negative and terminates at zero temperature before the termination of the T_{t} line at some negative D/J values. As Δ/J becomes positively larger, the critical lines are lowered in temperature, i.e., the TCPs are also seen at lower temperatures. Figure 2(c) is also the phase diagram obtained on the $(D/J, kT/J)$ planes for the given negative values of Δ/J with $z = 3$ and $h_{\mathrm{A}} = h_{\mathrm{B}} = 0.0$. As seen the critical lines are also lowered in temperature as Δ/J becomes more negative again. The TCPs are also seen at lower temperatures for lower negative Δ/J. We obtain that the highest temperatures are observed when $\Delta/J = 0.0$, and the temperatures are lowered by increasing $|\ \Delta/J\ |$.

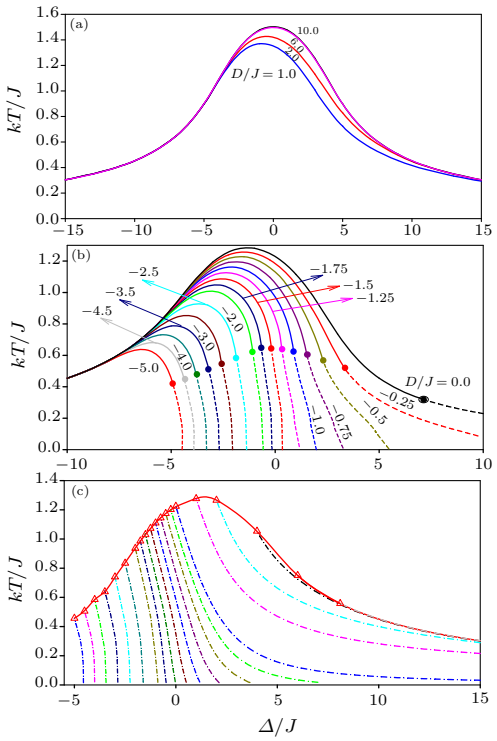

Fig. 3. Phase diagrams on $(\Delta/J, kT/J)$ planes for given D/J with $z = 3$. (a) Only T_{c} lines are observed when $D/J = 1.0$, 2.0, 6.0 and 10.0, (b) the T_{c}- and T_{t} lines combined at TCPs are found when $D/J = -0.25$, -0.5, -0.75, -1.0, -1.25, -1.5, -1.75, -2.0, -2.5, -3.0, -3.5, -4.0, -4.5 and -5.0, and (c) the lines of $T_{\mathrm{comp},Q}$ are shown for $D/J = 8.0$, 6.0, 4.0, 2.0, 1.0 0.0, -0.25, -0.5, -0.75, -1.0, -1.25, -1.5, -1.75, -2.0, -2.5, -3.0, -3.5, -4.0, -4.5 and -5.0. Triangles indicate the temperatures at which $T_{\mathrm{comp},Q}$ lines combine with T_{c} lines.

The next phase diagrams are given on the $(\Delta/J, kT/J)$ planes for given values of D/J. Figure 3(a) is obtained for positive values of D/J. As is seen, the T_{c} line is a very symmetric line with a

peak at $\Delta/J = 0.0$ and has the same shape at large values of D/J. It is clear that when $D/J = 6.0$ and 10.0 they are very close to each other. As D/J decreases, the symmetry is spoiled at large Δ. Our phase lines present similarities with the works such as Fig. 1 of Ref. [1], Fig. 2 of Ref. [3], Fig. 1(a) of Ref. [4], Fig. 1(c) of Ref. [28], Fig. 1(a) of Ref. [5] and Fig. 1 of Ref. [21]. Figure 3(b) is calculated for the negative D/J values including zero. As seen from the figure, we now have both T_c and T_t lines combined at the TCP for all D/J. It is clear that the TCP at the highest temperature is obtained for $D/J = -1.75$ about $\Delta/J = 0.0$. Away from these values the temperatures of TCPs decrease in both directions. The symmetry of Fig. 3(a) for higher positive D/J is totally spoiled. This kind of behavior is also observed in the works with Figs. 7 and 9 of Ref. [22], Fig. 1 of Ref. [20] and Fig. 2 of Ref. [29]. Figure 3(c) shows the thermal variations of the $T_{\mathrm{comp},Q}$ lines. The triangles indicate the connection points of these lines with the corresponding T_c lines. As $|\Delta/J|$ increases, they tend to disappear and the triangle maximum temperature is seen to be about $\Delta/J = 0.0$. The behavior of $T_{\mathrm{comp},Q}$ lines are overlooked because scientists so far have only concentrated on the behavior of $T_{comp,M}$ lines. However, $T_{\mathrm{comp},Q}$ lines may have an advantage over the $T_{comp,M}$ lines. That is, the existence of $T_{comp,M}$ requires mixed spins, but the existence of $T_{\mathrm{comp},Q}$ requires the addition of LCF and TCF into the system, which may be accomplished easily. In addition, they may have the same kind of practical usages in science and technology.

In conclusion, the thermodynamic properties of the mixed spin-1 and spin-1/2 Ising–Heisenberg model have been investigated on the honeycomb lattice with a new approach in the MF to examine the effects of TCF and LCF on the phase diagrams which are calculated on the $(\Delta/J, kT/J)$ and on the $(D/J, kT/J)$ planes by studying the thermal variations of magnetizations and quadrupole moments. It is found that the model yields both second and first-order phase transitions, and TCPs. The obtained phase diagrams have similar qualitative behaviors with the literature but overestimate the temperatures of the critical lines and the TCPs exist when $z = 3$ contrary to existing works. To overcome these problems, one may introduce a weight function $W(S_A, S_B; z)$, which should be inserted into the new approach, i.e., $z[M^z_{1/2}\hat{S}^z_{jB} + M^z_1\hat{S}^z_{iA}]$, in some way. This may lower the temperatures of the critical lines, thus it may lead to the disappearance of the TCPs when $z = 3$. Our next work will concentrate on finding such a weight function. In brevity, we have to say that the low temperature behavior of this work and previous works using the Oguchi approximations[10,11,17,18] are not successful at low temperatures. Lastly, the existences of $T_{\mathrm{comp},M}$ and $T_{\mathrm{comp},Q}$ are illustrated and the latter is studied in detail.

References

[1] Jiang W, Xiao G B, Wei G Z, Du A and Zhang Q 2004 *Commun. Theor. Phys.* **41** 131
[2] Belmamoun Y and Kerouad M 2008 *Phys. Scr.* **77** 025706
[3] Boughrara M and Kerouad M 2007 *Physica* A **374** 669
[4] Htoutou K, Ainane A and Saber M 2004 *J. Magn. Magn. Mater.* **269** 245
[5] Jiang W, Wei G Z and Du A 2002 *J. Magn. Magn. Mater.* **250** 49
[6] Xu C Q and Yan S L 2016 *J. Magn. Magn. Mater.* **416** 48
[7] Xu C Q and Yan S L 2013 *J. Magn. Magn. Mater.* **345** 261
[8] Wu H, Wei G, Zhang P, Yi G and Gong W 2010 *J. Magn. Magn. Mater.* **322** 3502
Wu H, Wei G, Du A, Yi G and Gong W 2011 *J. Magn. Magn. Mater.* **323** 1428
Wu H, Wei G and Yi G 2008 *Phys. Lett.* A **372** 6531
[9] Oitmaa J and von Brasch A M A 2003 *Phys. Rev.* B **67** 172402
[10] Bobák A, Pokorný V and Dely J 2009 *Physica* A **388** 2157
[11] Bobák A, Dely J and Žukovič M 2011 *Physica* A **390** 1953
[12] Čanová L and Strečka J 2010 *Phys. Status Solidi* B **247** 433
[13] Gálisová L and Strečka J 2011 *Condens. Matter Phys.* **14** 13002:1-11
[14] Hu A Y and Zhang A J 2016 *J. Magn. Magn. Mater.* **399** 22
[15] Čanová L, Strečka J and Lučivjanský T 2009 *Condens. Matter Phys.* **12** 353
[16] Hu A Y and Wang H Y 2016 *Mater. Res. Express* **3** 036105
[17] Albayrak E 2017 *J. Supercond. Novel Magn.* **30** 2555
Albayrak E 2017 *Physica* A **486** 161
[18] Bobák A, Pokorny V and Dely J 2010 *J. Phys.: Conf. Ser.* **200** 022001
[19] Mermin N D and Wagner H 1966 *Phys. Rev. Lett.* **17** 1133
[20] Jiang W, Wei G Z, Du A and Guo L Q 2002 *Physica* A **313** 503
[21] Eddeqaqi N C, Saber M, El-Atri A and Kerouad M 1999 *Physica* A **272** 144
[22] Carvalho D C and Plascak J A 2015 *Physica* A **432** 240
[23] Albayrak E and Keskin M 2003 *J. Magn. Magn. Mater.* **261** 196
[24] Gonçalves L L 1985 *Phys. Scr.* **32** 248
ibid 1986 *Phys. Scr.* **33** 192
[25] Da Silva N R and Salinas S R 1991 *Phys. Rev.* B **44** 852
[26] Buendia G M, Novotny M A and Zhang J 1994 *Springer Proceeds in Phys.* **78** 223
Buendia G M and Novotny M A 1997 *J. Phys.: Condens. Matter* **9** 5951
[27] De Resende H F V, Sa Barreto F C and Plascak J A 1988 *Physica* A **149** 606
[28] Bouhou S, Essaoudi I, Ainane A, Saber M, de Miguel J J and Kerouad M 2012 *Chin. Phys. Lett.* **29** 016101
[29] Costabile E, Viana J R, de Sousa J R and de Arruda A S 2015 *Solid State Commun.* **212** 30